Hierarchically porous NiO film grown by chemical bath deposition *via* a colloidal crystal template as an electrochemical pseudocapacitor material

Xin-hui Xia, Jiang-ping Tu,* Xiu-li Wang, Chang-dong Gu and Xin-bing Zhao

Received 23rd August 2010, Accepted 15th September 2010
DOI: 10.1039/c0jm02784g

Hierarchically porous NiO film has been successfully prepared by chemical bath deposition through monolayer polystyrene sphere template. The film possesses an architecture with a substructure of NiO monolayer hollow-sphere array and a superstructure of porous net-like NiO nanoflakes. The pseudocapacitive behavior of the NiO film is investigated by cyclic voltammograms (CV) and galvanostatic charge-discharge tests in 1 M KOH. The hierarchically porous NiO film exhibits weaker polarization, better cycling performance and higher specific capacitance in comparison with the dense NiO film. The specific capacitance of the porous NiO film is 309 F g^{-1} at 1 A g^{-1} and 221 F g^{-1} at 40 A g^{-1}, respectively, much higher than that of the dense NiO film (121 F g^{-1} at 1 A g^{-1} and 99 F g^{-1} at 40 A g^{-1}). The hierarchically porous architecture is responsible for the enhancement of electrochemical properties.

1. Introduction

Electrochemical capacitors (ECs), also called supercapacitors, have been an important development in the field of energy storage.[1–4] These devices have attracted great attention due to their higher power destiny, longer cycling life and faster recharge capability compared to secondary batteries.[1,2] Generally, ECs are classified into two types depending on the charge storage mechanism as well as the active materials used. (a) "Electrical double-layer capacitors", which exhibit a non-faradic reaction with accumulation of charges through electrostatic interactions at the electrode–electrolyte interface;[3] or (b) "pseudocapacitors" or "redox supercapacitors", which use fast and reversible surface or near-surface faradic reactions for charge storage.[5] Carbon-based active materials with high surface area are the most popular materials for electrical double-layer capacitors,[6–8] while transition metal oxides such as RuO_2, MnO_2 and NiO are considered to be the most promising pseudocapacitor candidate materials.[9–12] Though noble oxide RuO_2 could exhibit remarkably high specific capacitance values ranging from 720 to 760 F g^{-1} (for a single electrode system),[11,12] the high cost of these materials limits their commercial applications. Therefore, in the past decade, a great deal of effort has been devoted to searching for alternative inexpensive candidates with good capacitive characteristics similar to those of RuO_2.

Among the explored systems, NiO is a promising candidate for pseudocapacitors due to its easy availability, cost effectiveness, and good pseudocapacitive behavior.[3,5] It has been found that NiO could exhibit reversible pseudocapacitance about three times larger than those of active carbon materials (about 110 F g^{-1}),[13,14] which has greatly spurred the rapid development in this field. It is well accepted that pseudocapacitance is an interfacial phenomenon closely related to the morphology of electroactive materials. Research have demonstrated that the porous structure can provide a very short diffusion pathway for ion as well as a large active surface area, leading to enhanced electrochemical properties.[15] More recently, Wu *et al.*[16,17] reported several porous NiO films prepared by anodic electrodeposition and their improved pseudocapacitive performance over bulk counterparts. Thus, fabrication of films with porous structures is an effective way to enhance the pseudocapacitive performance.

Since it was first proposed by Nagayama *et al.*,[18] chemical bath deposition (CBD) has attracted considerable interest for preparing oxide films. The CBD process is a unique chemical route to produce nanostructured films in a "soft" manner. The method involves immersion of a substrate in an aqueous solution containing a precursor species. Then the desired oxides/hydroxides precipitate preferentially on the substrate surface, producing a conformal film. CBD is an advantageous technique due to its low cost, low temperature and as it is also convenient for large-area deposition. To date, various methods have been developed to prepare NiO films for pseudocapacitive application, including the sol–gel method,[19] electrodeposition,[20] sputtering,[21] high temperature solid-state method[22] and solvothermal synthesis.[23] However, there is little literature about the synthesis and application of porous NiO films *via* the CBD method for pseudocapacitors. On the other hand, colloidal monolayer lithography (typically polystyrene or silica spheres as the template) has proven to be a promising strategy for the fabrication of various ordered macroporous films because of its flexibility and controllable morphologies.[24–27] Hence, it would be interesting to combine the CBD method and colloidal monolayer template to prepare hierarchically porous NiO films for pseudocapacitors. Previously, our group has developed a facile and high-efficiency CBD method for fabricating highly porous NiO films.[28] In the present work, we report a hierarchically porous NiO film prepared by combining a self-assembled monolayer polystyrene (PS) sphere template and the CBD method. Remarkably, the as-prepared porous NiO film exhibits superior

State Key Laboratory of Silicon Materials and Department of Materials Science and Engineering, Zhejiang University, Hangzhou, 310027, China. E-mail: tujp@zju.edu.cn; Fax: +(86)-571-87952856; Tel: +(86)-571-87952573

pseudocapacitive performance with excellent capacity retention and high-rate capacity during cycling and thus has promising applications.

2. Experimental

2.1 Chemical materials

All solvents and chemicals were of reagent quality and were used without further purification. The monodispersed polystyrene (PS) spheres with three particle sizes (1 μm, 600 nm and 200 nm in diameter) were purchased from Alfa Aesar Corporation. They were well dispersed in deionized water and prepared as a suspension with a concentration of 2.5 wt. % before fabricating colloidal monolayers. The nickel sulfate, potassium persulfate and ammonia (25–28%) were obtained from Shanghai Chemical Reagent Co. All aqueous solutions were freshly prepared with high purity water (18 MΩ cm resistance).

2.2 Preparation of hierarchically porous NiO film

The monolayer PS sphere template was prepared as follows. Firstly, 5 drops of PS sphere suspension were dropped onto the surface of clean nickel foil substrate with a size of 2 × 2 cm^2. After holding the substrate stationary for 1 min to obtain good dispersion of the suspension, the substrate was then slowly immersed into deionized water. Once the suspension contacted the water's surface, a monolayer of PS spheres was observed on the surface of the water and on the surface of the nickel foil substrate. To prevent any further additions to the substrate, it was kept immersed. Then, a few drops of 2% dodecylsodiumsulfate solution were added to the water to change the surface tension. As a result, the monolayer of PS spheres that were suspended on the surface of the water was pushed aside due to the change in the surface tension. Then the substrate was lifted up through the clear area, making sure that no additional PS spheres were deposited on the monolayer during this process and followed by heating at 110 °C in an oven for 5 min to bond the monolayer with the nickel foil substrate.

The solution for the chemical bath deposition was obtained by mixing 80 ml of 1 M nickel sulfate, 60 ml of 0.25 M potassium persulfate and 20 ml of aqueous ammonia (25–28%) in a 250 ml pyrex beaker at room temperature. The above templated substrate was used in this work. Its back side was protected from solution contamination by uniformly coating with polyimide tape. The substrate was placed vertically in the freshly resulting solution, and was kept at 25 °C for 30 min to deposit the precursor film. The reactions involving in the CBD method occur as follows:[28]

$$[Ni(H_2O)_{6-x}(NH_3)_x]^{2+} + 2OH^- \rightarrow Ni(OH)_2 + (6-x)H_2O + xNH_3 \quad (1)$$

$$2Ni(OH)_2 + S_2O_8^{2-} \rightarrow 2NiOOH + 2SO_4^{2-} + 2H^+ \quad (2)$$

Then the precursor film was washed with deionized water. After removing the tape masks, it was immersed in toluene for 24 h to remove the PS sphere template. Finally, the precursor film was annealed at 350 °C in argon for 1.5 h.

For the sake of comparison, a porous NiO film without the PS sphere template was prepared as the same CBD deposition parameters detailed above. Meanwhile, a dense NiO film was also prepared without template by a cathodic electrodeposition method, which was carried out at constant current of 2.0 mA cm^{-2} for 500 s in aqueous solution containing 1 M $Ni(NO_3)_2$ and 0.075 M $NaNO_3$. The deposition of precursor film includes an electrochemical reaction and a precipitation reaction expressed as follows:[29]

$$NO_3^- + H_2O + 2e^- \rightarrow NO_2^- + 2OH^- \quad (3)$$

$$Ni^{2+} + 2OH^- \rightarrow Ni(OH)_2 \quad (4)$$

The film was also annealed at 350 °C in argon for 1.5 h. The thickness of both NiO films was approximately 1.1 μm. The loading weight for CBD and electrodeposited NiO films is 1.2 and 1.4 mg cm^{-2}, respectively.

2.3 Characterization

The precursor film and the annealed films were characterized by X-ray diffraction (XRD, Philips PC-APD with Cu-Kα radiation). The morphologies of all films were observed by field emission scanning electron microscopy (FESEM, FEI SIRION) and transmission electron microscopy (TEM, JEM 200 CX 160 kV). The surface area of the film power scratched from the substrate was determined by BET (Brunauer-Emmett-Teller) measurements using a NOVA-1000e surface area analyzer.

The electrochemical measurements were carried out in a three electrode electrochemical cell containing 1 M KOH aqueous solution as the electrolyte. Cyclic voltammetry (CV) measurements and electrochemical impedance spectroscopy (EIS) tests were performed on a CHI660c electrochemical workstation (Chenhua, Shanghai). CV measurements were carried out at a scanning rate of 10 mV s^{-1} between 0.1 V and 0.65 V at 25 °C, with the NiO film as the working electrode, Hg/HgO as the reference electrode and a Pt foil as counter-electrode. EIS tests were made with a superimposed 5 mV sinusoidal voltage in the frequency range of 100 kHz–0.01 Hz. The EIS results obtained experimentally were analyzed using a nonlinear least squares fitting program EQUIVCRT. The galvanostatic charge-discharge tests were conducted on a LAND battery program-control test system. The as-prepared electrodes, together with a nickel mesh counter electrode and an Hg/HgO reference electrode were tested in a three-compartment system.

3. Results and discussion

3.1 Synthesis and characterization of hierarchically porous NiO film

XRD patterns of films prepared by the CBD method and electrodeposition are shown in Fig. 1. Excluding three strong peaks from the nickel foil substrate, the peaks at 37.2, 43.3, and 62.8° in both patterns can be indexed as (111), (200) and (220) crystal planes of cubic NiO phase (JCPDS 4–0835), respectively, indicating that the NiO films have formed through the decomposition of precursor films after heat treatment. For the NiO film prepared with the PS sphere template, the diffraction peaks of

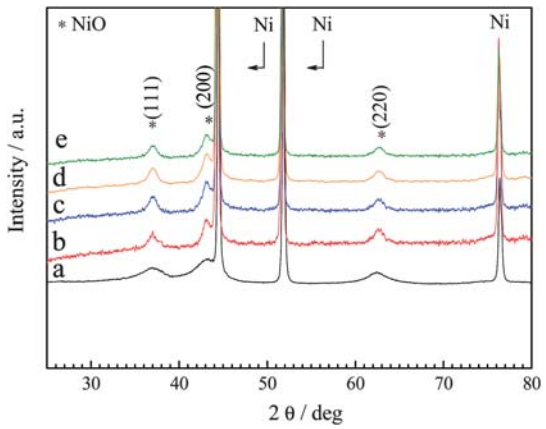

Fig. 1 XRD patterns of films prepared by CBD method with PS sphere template (a) 1 μm sphere; (b) 600 nm sphere; (c) 200 nm sphere; (d) film prepared by CBD method without PS sphere template; (e) dense NiO film prepared by electrodeposition.

film obtained with 1 μm PS sphere are broader than those obtained by PS sphere with 600 and 200 nm in diameter. It is also observed that the intensities of these peaks increase as the PS sphere particle size decreases, indicating that the film prepared with smaller PS spheres has better crystallinity.

Fig. 2 presents SEM images of a monolayer PS sphere template for hierarchically porous NiO film. In our case, the PS spheres with three different particle size (1 μm, 600 and 200 nm) are all well-organized into a long-range hexagonal close-packed alignment perpendicular to the nickel foil substrate. Hierarchically porous NiO film is successfully prepared after removing the PS sphere template in combination with heat treatment. Taking 1 μm PS sphere for example, note that the as-prepared NiO film has a typical hierarchically porous structure consisting of two parts (Fig. 3a and b). The substructure of the film is composed of a monolayer close-packed hollow-sphere with a diameter of 1 μm (Fig. 3a and b). The superstructure is uniformly covered with a thin film of free-standing NiO nanoflakes with a thickness of about 30 nm (Fig. 3b). Additionally, the NiO nanoflakes arrange vertically to the monolayer NiO hollow-sphere array (Fig. 3a). The NiO nanoflakes are interconnected to each other resulting in the formation of extended network structures with pore diameters of 30–300 nm.

The hierarchically porous structure can be more clearly observed when the film is detached from the substrate by a blade. The bottom of the detached film shows an ordered bowel-like array (Fig. 3c) and the leaf part on the substrate is a corresponding bowl-like array layer (Fig. 3d). The hierarchical pore system is also proved by the TEM images. The segment separated from the porous NiO film exhibits a typical circle structure connected with nanoflakes (Fig. 3e), which is consistent with the results from the SEM images. Moreover, the individual nanoflake is thin and flat with low-roughness (Fig. 3f). In addition, all the diffraction rings in the selected area electronic diffraction (SAED) patterns can be assigned to the cubic NiO phase (JCPDS 4–0835), indicating that the films are polycrystalline in nature, which is in agreement with the XRD result. Based on these patterns, it is justified that the as-prepared NiO film has a typical hierarchical porous structure. Meanwhile, a similar hierarchically porous structure is also obtained for the PS sphere at 600 and 200 nm in diameter, respectively (Fig. 4a and b).

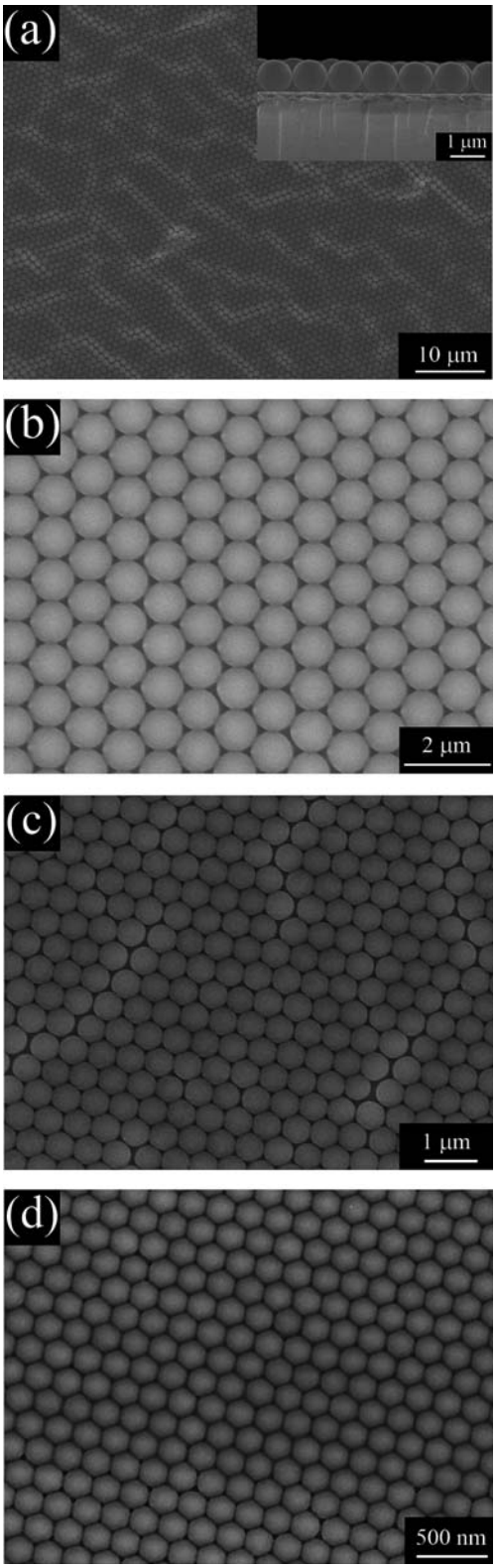

Fig. 2 SEM images of the monolayer PS sphere template assembled by (a), (b) 1 μm PS sphere (side view presented in inset); (c) 600 nm PS sphere; (d) 200 nm PS.

The NiO thin film prepared by CBD without a PS sphere template exhibits a highly porous net-like structure constructed of many interconnected nanoflakes with a thickness of 30 nm

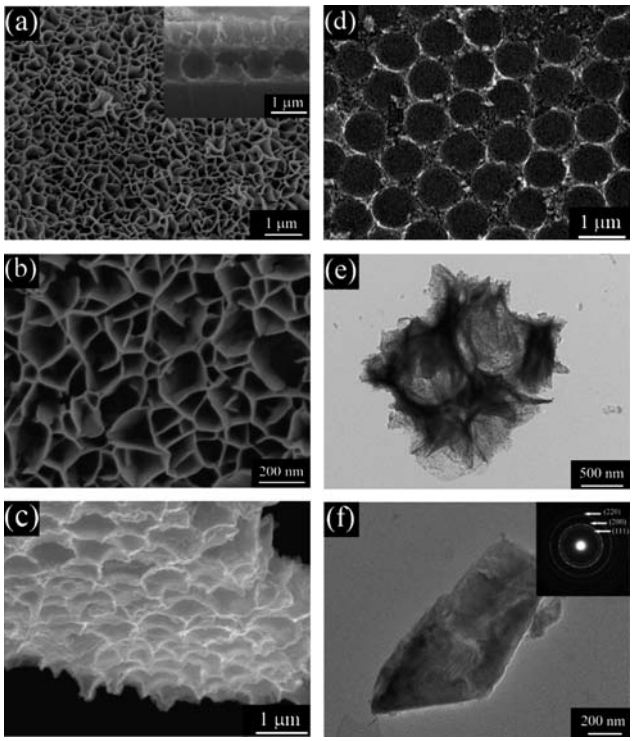

Fig. 3 Morphological and structural characterizations of hierarchically porous NiO film prepared by 1μm PS sphere: (a), (b) SEM images of top and side views (side view presented in inset); (c) typical SEM image of the film detached from the substrate; (d) the residual pattern left on the substrate; (e), (f) TEM images (SAED pattern presented in inset).

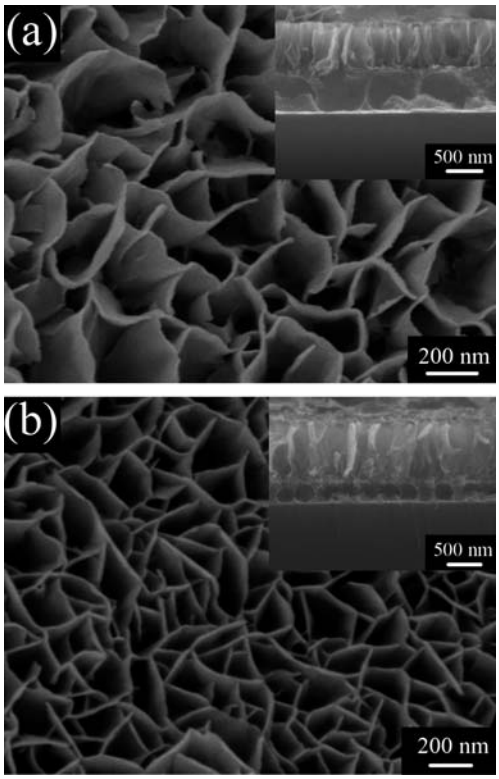

Fig. 4 SEM images of a hierarchically porous NiO film prepared by (a) 600 nm PS sphere and (b) 200 nm PS sphere. The upper-right insets in (a) and (b) correspond to side views of the films.

(Fig. 5a and b). The nanoflakes are arranged vertically to the substrate, forming a net-like structure and leaving pores of 30–300 nm. The film prepared by eletrodeposition, however, exhibits a homogeneous dense structure (Fig. 6a). The flake from the dense film presents a rough appearance with nanoparticles (Fig. 6b and c). The SAED pattern is similar to those of Fig. 3f and Fig. 5c, also displaying a crystalline structure (Fig. 6c).

The hierarchical pore system in the NiO film obtained by the CBD method may bestow the possibility of combining the different functionality provided by each type of porosity. The macropores in the monolayer hollow-sphere array can absorb and strongly retain electrolyte ions, ensuring sufficient faradic reactions, especially at high current densities. The net-like porous superstructure can afford high specific surface area for electrochemical energy storage. Thus, it is believed that this hierarchically porous structure is beneficial to the enhancement of pseudocapacitive performance.

3.2 Electrochemical analysis

Electrochemical capacitor properties of all films are elucidated by cyclic voltammograms (CV) and galvanostatic charge-discharge tests. Fig. 7 shows the discharge profiles of NiO films prepared by the CBD method with a PS sphere template at a galvanostatic current density of 1 A g^{-1}. Their specific capacitance can be calculated according to the following equation:

$$C = \frac{I\,\Delta t}{M\Delta V} \quad (5)$$

where C (F g^{-1}) is specific capacitance, I (mA) represents discharge current, and M (mg), ΔV (V) and Δt (sec) designate the mass of the active materials, potential drop during discharge and total discharge time, respectively. Three hierarchically porous NiO films prepared with different PS sphere size exhibit pseudocapacitances of 309 F g^{-1} for 1 μm PS sphere, 312 F g^{-1} for 600 nm PS sphere and 310 F g^{-1} for 200 nm PS sphere, respectively, indicating that the PS sphere size does not has an obvious effect on the pseudocapacitance of the hierarchically porous NiO film. Therefore, we select the NiO film prepared with the 1 μm PS sphere as a representative to investigate the pseudocapacitive behavior in detail.

Fig. 8 shows the typical CV curves of three film electrodes at a scan rate of 10 mV s^{-1}. The experiment results describing the features of the CVs are presented in Table 1 in detail. The CV curves for the three film electrodes are quite similar and only one redox couple is observed, represented by the following electrochemical reaction:[28,30]

$$NiO + OH^- \leftrightarrow NiOOH + e^- \quad (6)$$

The charge process of the film is associated with the oxidation peak before oxygen evolution (OE), whereas the discharge process is associated with the reduction peak. Obviously, the peak currents of both porous films are much higher than those of the dense film, indicating that the porous NiO film has higher electrochemical reaction activity. Besides, both porous NiO films show lower oxidation potential and higher reduction potential

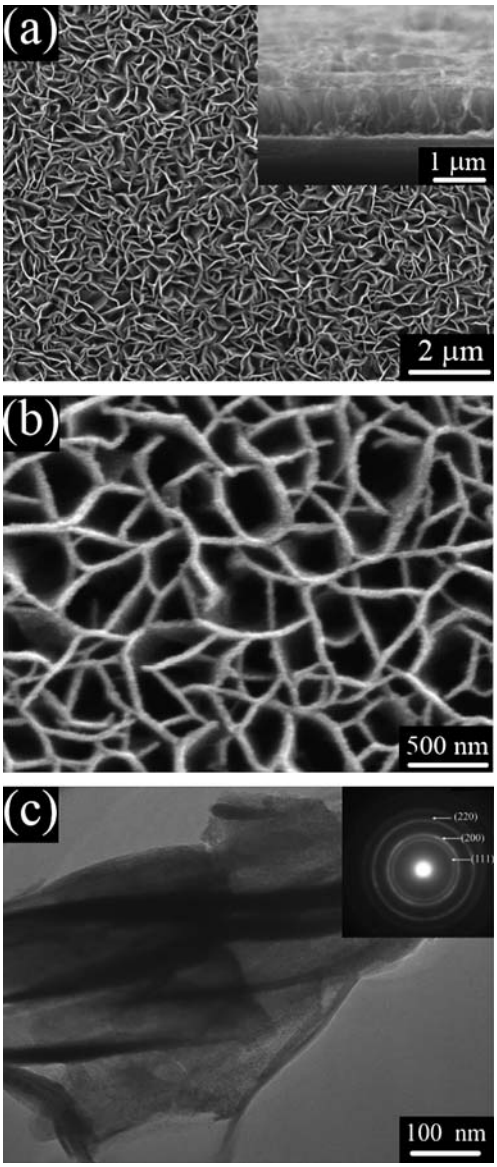

Fig. 5 Morphological and structural characterizations of the dense NiO film: (a) SEM images of top and side views (side view presented in inset); (b), (c) TEM images (SAED pattern presented in inset).

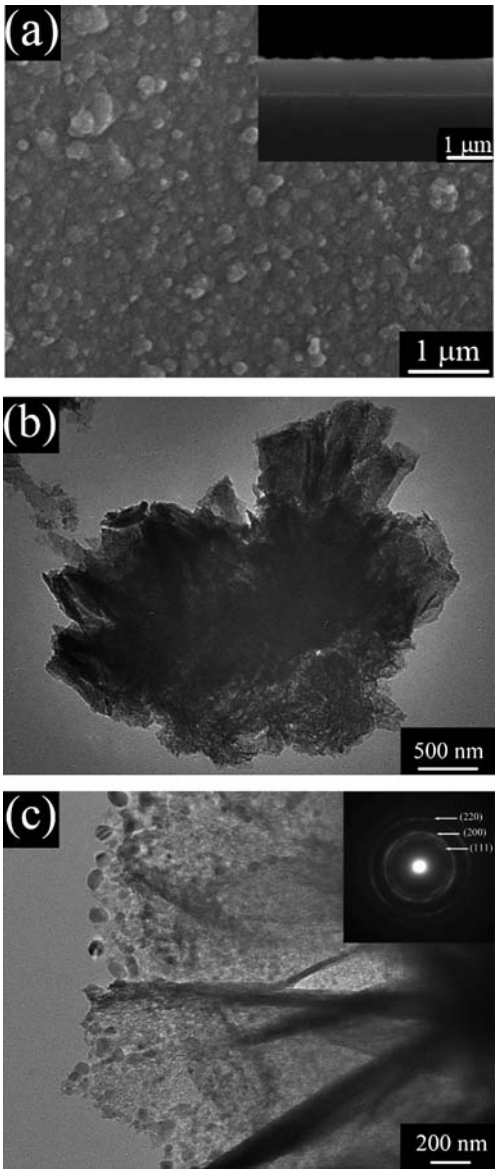

Fig. 6 Morphological and structural characterizations of the dense NiO film: (a) SEM images of top and side views; (b), (c) TEM images (SAED pattern presented in inset).

than the dense film at the same rates, and shorten the potential separation between the oxidation peak and the reduction peak. It is suggested that both porous films have weaker polarization, better electrochemical activity and reaction reversibility. Furthermore, the hierarchically porous NiO film prepared with the PS sphere template shows almost the same oxidation and reduction peak potentials as those of porous NiO prepared without the PS sphere template, as well as slightly lower peak current intensities.

Fig. 9a shows the first charge-discharge profiles of three NiO film electrodes between 0 and 0.55 V (*vs.* Hg/HgO) at a galvanostatic current density of 1 A g^{-1}. The shape of the charge-discharge curves presents typical pseudocapacitive behavior, which is in agreement with the CV result. The specific capacitance values for the hierarchically porous, porous and dense NiO films are 309 F g^{-1}, 311 F g^{-1} and 121 F g^{-1}, respectively. Furthermore, both porous NiO films exhibit a much lower charge voltage plateau and higher discharge voltage plateau than the dense film, indicating that the porous film electrode has smaller polarization during the charge-discharge processes. Moreover, the porous NiO prepared without the PS sphere template presents the smallest polarization. Both porous NiO films possess quite good pseudocapacitance at different discharge current densities. The hierarchically porous NiO film prepared with the PS sphere template exhibits pseudocapacitance of 309 F g^{-1} at 1 A g^{-1}, 270 F g^{-1} at 2 A g^{-1}, 253 F g^{-1} at 4 A g^{-1}, 224 F g^{-1} at 10 A g^{-1}, 223 F g^{-1} at 20 A g^{-1} and 221 F g^{-1} at 40 A g^{-1}, respectively (Fig. 9b). These values are comparable to those obtained from the porous NiO prepared without PS sphere template (311 F g^{-1} at 1 A g^{-1}, 273 F g^{-1} at 2 A g^{-1}, 256 F g^{-1} at

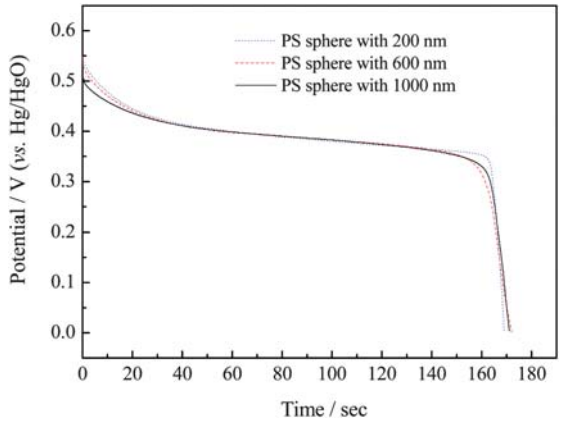

Fig. 7 The first discharge profiles of three NiO films prepared with different PS sphere size at a current destiny of 1 A g^{-1}.

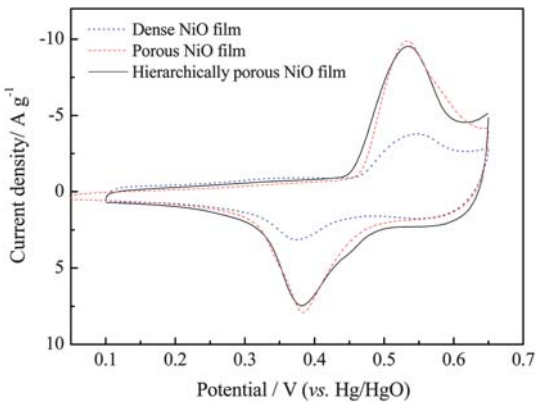

Fig. 8 CV curves of the three NiO film electrodes in the potential region of 0.1–0.65 V at a scanning rate of 10 mV s^{-1} at the first cycle.

4 A g^{-1}, 226 F g^{-1} at 10 A g^{-1}, 225 F g^{-1} at 20 A g^{-1} and 223 F g^{-1} at 40 A g^{-1}, respectively, see Fig. 9c). But the dense film exhibits much lower pseudocapacitance with 121 F g^{-1} at 1 A g^{-1}, 109 F g^{-1} at 2 A g^{-1}, 105 F g^{-1} at 4 A g^{-1}, 101 F g^{-1} at 10 A g^{-1}, 100 F g^{-1} at 20 A g^{-1} and 99 F g^{-1} at 40 A g^{-1}, respectively (Fig. 9d). The remarkable improvement of the pseudocapacitance of porous NiO films is due to the unique hierarchical porous architecture. First, the free-standing NiO nanoflakes with open spaces allow easy diffusion of ions among them and shorten the diffusion paths for both electrons and ions within the oxides. Second, the macropores in the monolayer hollow-sphere array can absorb and strongly retain the electrolyte, ensuring efficient contact between active materials and electrolytes. Third, the porous

Table 1 Characteristic parameters for the CVs of the three NiO film electrodes (corresponding to Fig. 8)

Film electrode	Anode peak potential/mV	Cathode peak potential/mV	Peak potential separation/mV
Hierarchically Porous NiO film	532	386	144
Porous NiO film	532	384	142
Dense NiO film	555	371	184

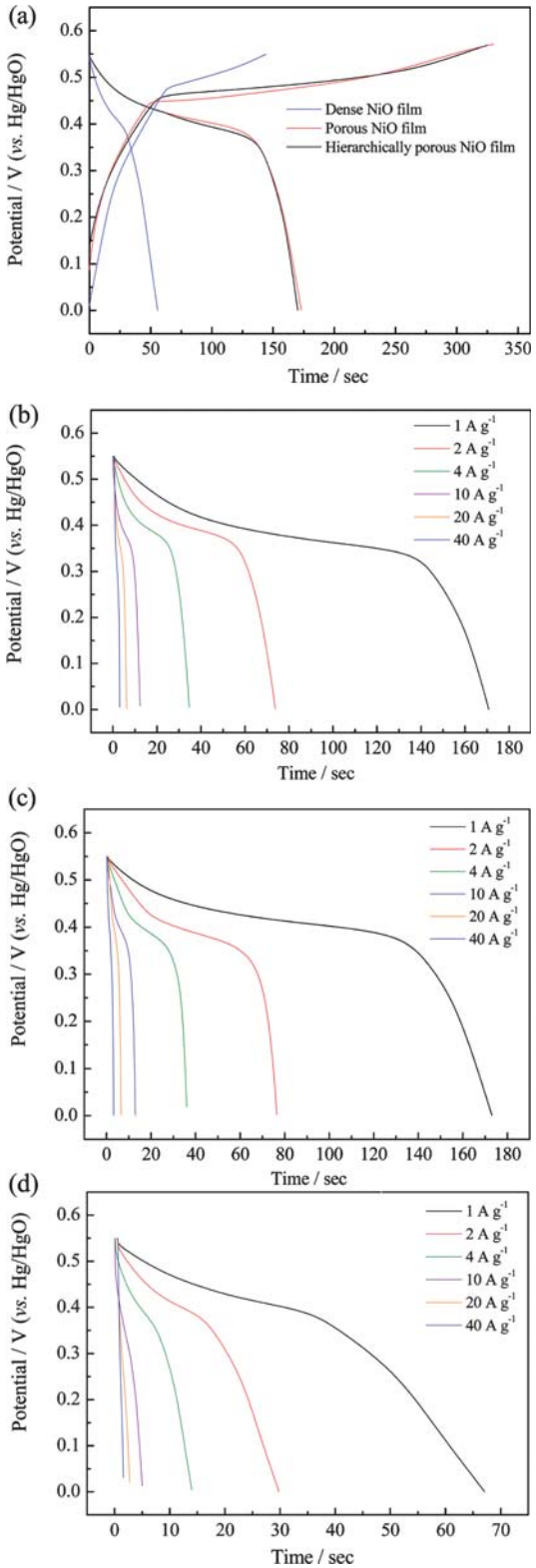

Fig. 9 (a) The first charge-discharge profiles of the three NiO film electrodes at a current destiny of 1 A g^{-1}; (b) discharge curves of the hierarchically porous NiO film at different discharge current densities; (c) discharge curves of the porous NiO film at different discharge current densities; (d) discharge curves of the dense NiO film at different discharge current densities.

structure provides larger surface area and more active sites for electrochemical reactions, supported by the BET results. The BET measurements (Fig. 10) show that the surface area of hierarchically porous, porous and dense NiO films is 290, 325 and 42 $m^2\ g^{-1}$, respectively. These features are particularly helpful for high rate applications, resulting in better pseudocapacitive performance. On the other hand, it should be noted that the high porosity will lead to the low volumetric capacity and low volumetric energy density of the electrode material.

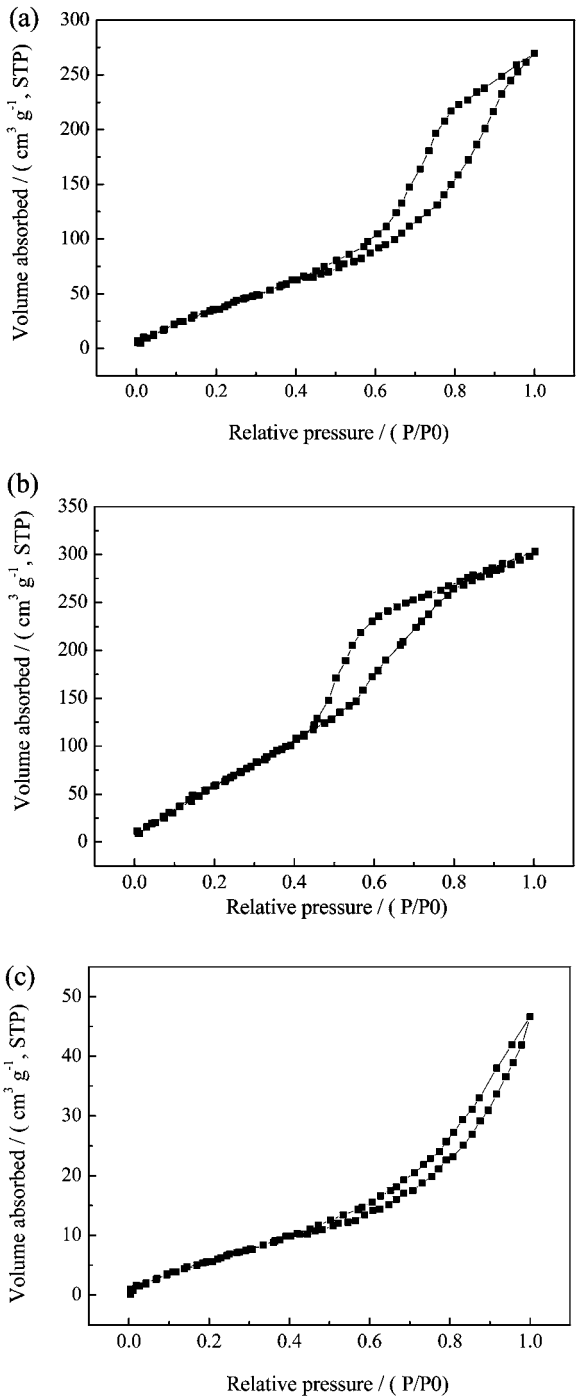

Fig. 10 BET measurements of the three NiO films: (a) hierarchically porous NiO film; (b) porous NiO film; (c) dense NiO film.

The EIS plots of the three film electrodes are presented in Fig. 11. All EIS curves are composed of a depressed arc in high frequency regions and a straight arc in low frequency regions. It is well accepted that the semicircle reflects the electrochemical reaction impedance of the film electrode and the straight line indicates the diffusion of the electroactive species.[31,32] A bigger semicircle means larger charge-transfer resistance, and higher slope signifies lower diffusion rate. It is noted that both porous NiO films exhibit a smaller semicircle and lower slope, indicating that both porous films have smaller charge transfer resistance and faster ion diffusion rate, which are consistent with the pseudocapacitive results above.

Fig. 12 presents the cycle characteristics of three NiO film electrodes by charge-discharge at a current density of 1 A g^{-1}. Upon cycling, the discharge pseudocapacitance increases up to 500 cycles and then decays slightly for ongoing cycles. The hierarchically porous film exhibits excellent pseudocapacitance retention with 315 F g^{-1} after 4000 cycles, maintaining 89% of the maximum value, higher than that of the porous NiO film (258 F g^{-1} with 72%), while the dense film only shows 96 F g^{-1} after 4000 cycles with 58% of the maximum value. After

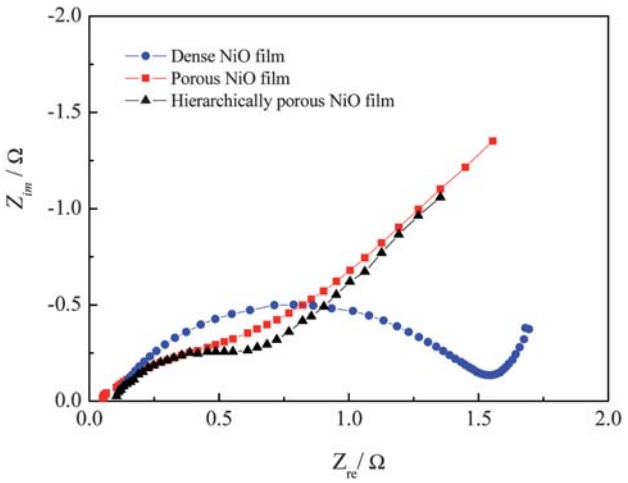

Fig. 11 EIS plots of the three NiO film electrodes at 100% depth of discharge.

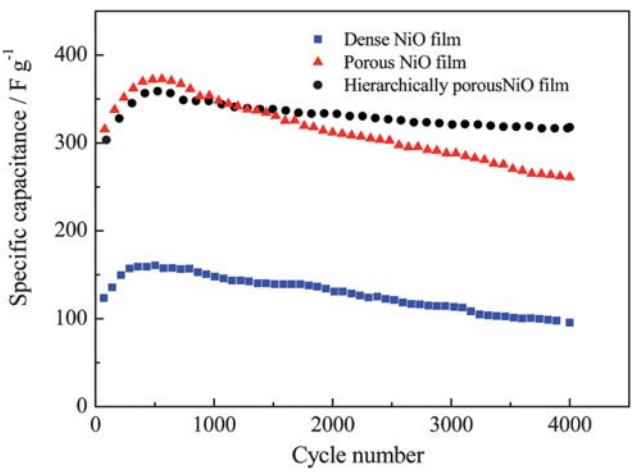

Fig. 12 Cycling performances of the three NiO film electrodes at 1 A g^{-1}.

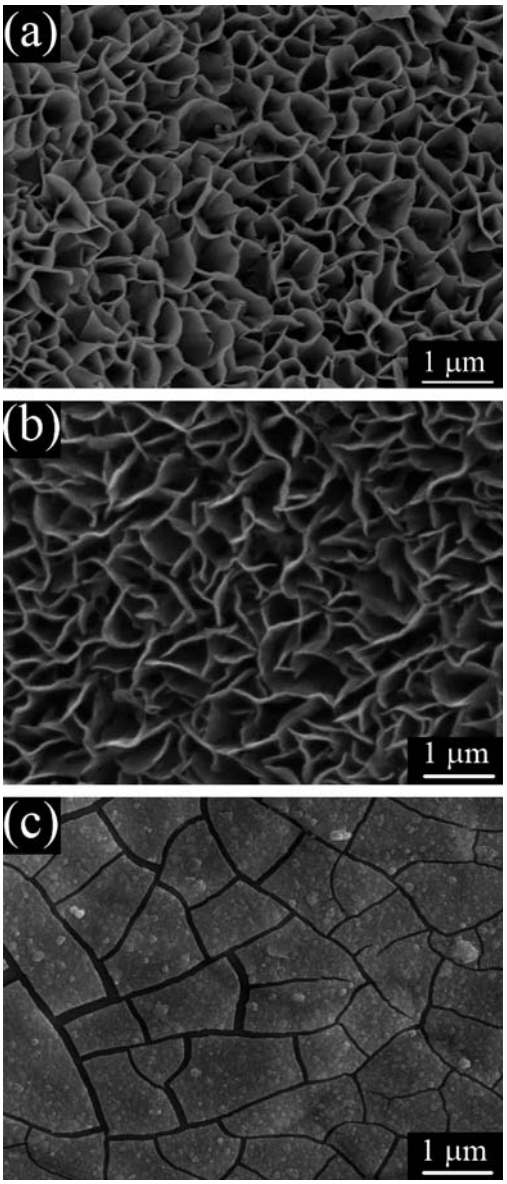

Fig. 13 SEM images of the fully charged (a) hierarchically porous NiO film; (b) porous NiO film; (c) dense NiO film electrodes after 4000 cycles.

4000 cycles, both porous NiO films maintain the porous structure integrity (Fig. 13a and b), while the dense film is disintegrated and leaves many cracks in the film (Fig. 13c). The hierarchically porous structure could alleviate the structure damage caused by volume expansion during the cycling process and keep the structure stable, resulting in better cycling performance. It is also noted that the hierarchically porous NiO film prepared with the PS sphere template exhibits superior cycling stability to the porous NiO film without PS sphere template. These results are also confirmed by the CV test. Fig. 14 shows the CV curves of the three NiO films obtained after 4000 charge-discharge cycles at 1 A g^{-1}. The oxidation and reduction peaks of all the films shift to higher and lower potentials respectively, leading to a larger potential separation between the oxidation and the reduction peak, indicating that the reaction reversibility becomes worse as the cycle proceeds. Even so, the hierarchically porous NiO film exhibits the smallest peak potential separation and the highest

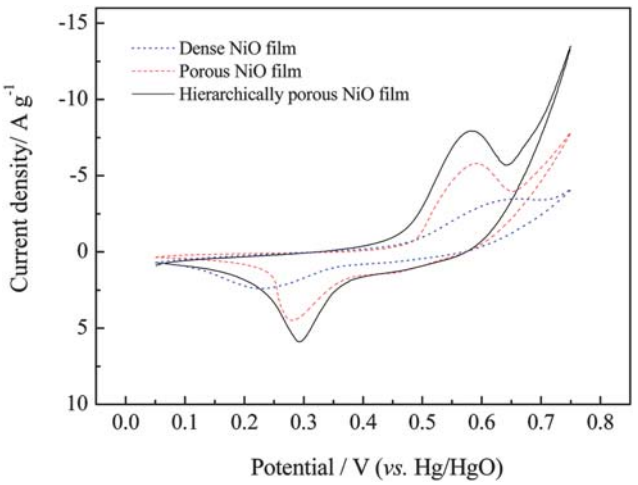

Fig. 14 Cyclic voltammograms of the three NiO films obtained after 4000 charge-discharge cycles at 1 A g^{-1}.

Table 2 Characteristic parameters for the CVs of the three NiO film electrodes after 4000 charge-discharge cycles at 1 A g^{-1} (corresponding to Fig. 15)

Film electrode	Anode peak potential/mV	Cathode peak potential/mV	Peak potential separation/mV
Hierarchically Porous NiO film	582	293	298
Porous NiO film	596	278	318
Dense NiO film	648	218	430

current intensities (Table 2), but the dense film shows much bigger potential separation and lower current intensities, meaning that the hierarchically porous NiO film has the best reactivity and reaction reversibility after 4000 cycles, which is in agreement with the cycling result.

The improved cycling stability is due to the hierarchically porous structure, which could hinder the degradation of NiO more effectively. The degradation mechanism of the NiO film is a complex process, mainly associated with two factors: a self-discharge phenomenon associated to a partial dissolution of NiO and oxygen bubbles striking. The pseudocapacitive process of NiO is a faradaic process based on the well-known NiO/NiOOH two-phase system, accompanied by a spontaneous chemical conversion of NiO in $Ni(OH)_2$ at the electrode/electrolyte interface. This NiO/$Ni(OH)_2$ process leads to a progressive degradation of the pseudocapacitive performances of Ni(II)/Ni(III) couple (Fig. 15). Besides, the oxygen evolution reaction is in competition with the electrochemical process of the Ni(II)/Ni(III) couple during the cycle. The oxygen bubbles strike the film accelerating the degradation process. As illustrated above, for the porous NiO film prepared without the PS sphere template, the NiO nanoflakes are arranged vertically to the substrate, meaning that the direct contact area between an individual nanoflake and the substrate is about 30 nm. During the cycling, a partial dissolution of the root of the NiO nanoflake will result in structural fragility. Meanwhile, the oxygen bubbles formed by the oxygen evolution reaction strike the film accelerating

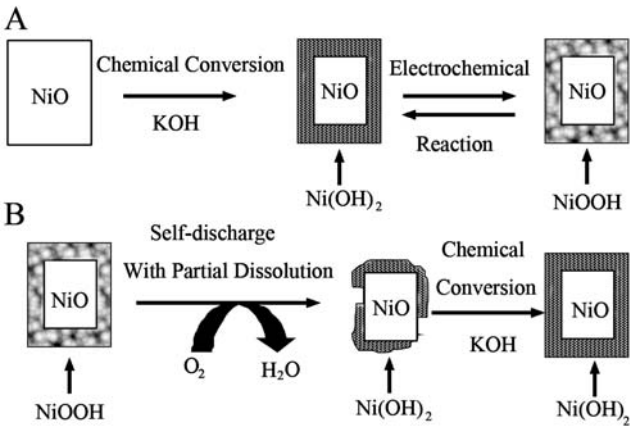

Fig. 15 The degradation mechanism of the NiO film.

the degradation process, even causing electrode breakdown. However, for the hierarchically porous NiO film prepared with the PS sphere template, the substructure of the film is composed of a monolayer close-packed hollow-sphere array, which has bigger contact area with the substrate, and the individual hollow-spheres are tightly connected with each other, allowing it to resist the bubble striking more effectively. The interaction of all these factors leads to slow degradation and better cycling stability.

4. Conclusion

In summary, a hierarchically porous NiO film is prepared by the combination of the CBD method and a monolayer polystyrene sphere template. The film possesses a structure consisting of two parts: the superstructure is porous net-like NiO nanoflakes and the substructure is a NiO monolayer hollow-sphere array. Compared to the dense NiO film, the hierarchically porous film exhibits superior pseudocapacitive performance with higher specific pseudocapacitance and better cycling performance. A specific pseudocapacitance of 309 F g^{-1} is obtained for the hierarchically porous film. Meanwhile, the porous film shows weaker polarization and better reversibility. The enhanced electrochemical capacitive performance is mainly due to the high porosity and large surface area of the hierarchically porous architecture. Additionally, the hierarchically porous can effectively hinder NiO degradation resulting in better cycling stability.

References

1 B. E. Conway, *J. Electrochem. Soc.*, 1991, **138**, 1539.
2 J. R. Miller and P. Simon, *Science*, 2008, **321**, 651.
3 P. Simon and Y. Gogotsi, *Nat. Mater.*, 2008, **7**, 845.
4 J. Y. Huang, K. Wang and Z. X. Wei, *J. Mater. Chem.*, 2010, **20**, 1117.
5 Y. Zhang, H. Feng, X. B. Wu, L. Z. Wang, A. Q. Zhang, T. C. Xia, H. C. Dong, X. F. Li and L. S. Zhang, *Int. J. Hydrogen Energy*, 2009, **34**, 4889.
6 H. J. Liu, W. J. Cui, L. H. Jin, C. X. Wang and Y. Y. Xia, *J. Mater. Chem.*, 2009, **19**, 3661.
7 H. J. Liu, X. M. Wang, W. J. Cui, Y. Q. Dou, D. Y. Zhao and Y. Y. Xia, *J. Mater. Chem.*, 2010, **20**, 4223.
8 S. W. Woo, K. Dokko, H. Nakano and K. Kanamura, *J. Mater. Chem.*, 2008, **18**, 1674.
9 K. Konstantinov, G. X. Wang, Z. J. Lao, H. K. Liu and T. Devers, *J. Nanosci. Nanotechnol.*, 2009, **9**, 1263.
10 R. R. Jiang, T. Huang, J. L. Liu, J. H. Zhuang and A. S. Yu, *Electrochim. Acta*, 2009, **54**, 3047.
11 S. H. Oh and L. F. Nazar, *J. Mater. Chem.*, 2010, **20**, 3834.
12 Y. B. Xie and D. G. Fu, *Mater. Chem. Phys.*, 2010, **122**, 23.
13 F. B. Zhang, Y. K. Zhou and H. L. Li, *Mater. Chem. Phys.*, 2004, **83**, 260.
14 M. W. Xu, S. J. Bao and H. L. Li, *J. Solid State Electrochem.*, 2007, **11**, 372.
15 X. H. Xia, J. P. Tu, J. Zhang, X. L. Wang, W. K. Zhang and H. Huang, *Electrochim. Acta*, 2008, **53**, 5721.
16 M. S. Wu, C. Y. Huang and K. H. Lin, *J. Power Sources*, 2009, **186**, 557.
17 M. S. Wu, M. J. Wang and J. J. Jow, *J. Power Sources*, 2010, **195**, 3950.
18 H. Nagayama, H. Honda and H. Kawahara, *J. Electrochem. Soc.*, 1988, **135**, 2013.
19 K. C. Liu and M. A. Anderson, *J. Electrochem. Soc.*, 1996, **143**, 124.
20 V. Srinivasan and J. W. Weidner, *J. Electrochem. Soc.*, 1997, **144**, L210.
21 S. H. Lee, C. E. Tracy and J. R. Pitts, *Electrochem. Solid-State Lett.*, 2004, **7**, A299.
22 Y. Zhang, Y. G. Gui, X. B. Wua, H. Feng, A. Q. Zhang, L. Z. Wang and T. C. Xia, *Int. J. Hydrogen Energy*, 2009, **34**, 2467.
23 T. Nathan, A. Aziz, A. F. Noor and S. R. S. Prabaharan, *J. Solid State Electrochem.*, 2008, **12**, 1003.
24 P. N. Bartlett, J. J. Baumberg, P. R. Birkin, M. A. Ghanem and M. C. Netti, *Chem. Mater.*, 2002, **14**, 2199.
25 M. Sadakane, T. Horiuchi, N. Kato, C. Takahashi and W. Ueda, *Chem. Mater.*, 2007, **19**, 5779.
26 L. J. Fu, T. Zhang, Q. Cao, H. P. Zhang and Y. P. Wu, *Electrochem. Commun.*, 2007, **9**, 2140.
27 L. J. Fu, L. Yang, Y. Shi, B. Wang and Y. P. Wu, *Microporous Mesoporous Mater.*, 2009, **117**, 515.
28 X. H. Xia, J. P. Tu, J. Zhang, X. L. Wang, W. K. Zhang and H. Huang, *Sol. Energy Mater. Sol. Cells*, 2008, **92**, 628.
29 G. Duan, W. Cai, Y. Luo and F. Sun, *Adv. Funct. Mater.*, 2007, **17**, 644.
30 M. Chigane and M. Ishikawa, *J. Electrochem. Soc.*, 1994, **141**, 3439.
31 A. H. Zimmerman and P. K. Effa, *J. Electrochem. Soc.*, 1984, **131**, 709.
32 R. D. Armstrong and H. Wang, *Electrochim. Acta*, 1991, **36**, 759.